Variable Spacetime Impedance

A Stochastic Vacuum Framework (SVF)

Grant Lindblom

Figure 4.1: The Proton as a Topological Trefoil Knot

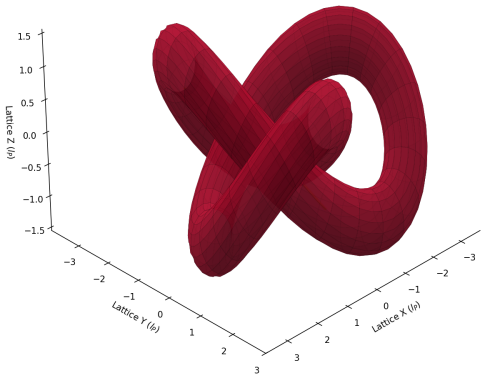

February 10, 2026

Abstract

Theoretical physics has reached a juncture where the mathematical complexity of our models has outpaced our mechanical understanding. This text proposes a return to hardware: treating the vacuum not as a geometric abstraction, but as a **Discrete Amorphous Manifold (M_A)** governed by finite inductive and capacitive limits. From this substrate, we derive Inertia, Gravity, and Mass as emergent engineering properties of a tunable transmission medium.

Contents

Preface

Theoretical physics has reached a juncture where the mathematical complexity of our models has outpaced our mechanical understanding of the phenomena they describe. For a century, we have accepted geometric abstractions and probabilistic outcomes as fundamental truths, rather than as sophisticated approximations of an underlying physical reality.

Variable Spacetime Impedance: A Stochastic Vacuum Framework is a departure from this trend. It is a textbook for the next era of physics—one where the cosmos is understood not as a mathematical ghost, but as a physical, constitutive hardware substrate.

The Shift from Geometry to Hardware

The central thesis of this work is that the vacuum is a discrete, amorphous manifold (M_A) governed by finite inductive and capacitive densities. By redefining the fundamental constants of nature as the bulk engineering properties of this substrate, we move from a descriptive physics to an operational one.

In this framework:

- **Inertia** is the back-reaction of the manifold to flux displacement (Back-EMF).
- **Gravity** is the refractive consequence of localized metric strain.
- **Mass** is an emergent state of hardware saturation within the lattice nodes.

Pedagogical Approach

This text is structured as a layered "stack," progressing from the raw physical substrate to macroscale astrophysical observations:

1. **Part I (The Substrate):** Establishes the nodal geometry and the laws governing signal propagation within the manifold.
2. **Part II (Emergence):** Derives the "Quantum" and "Weak" interactions as deterministic results of chiral bias and bandwidth limits.
3. **Part III (Macroscale):** Applies these local hardware limits to galactic rotation and cosmic evolution, providing a particle-free alternative to Dark Matter and Dark Energy.
4. **Part IV (Verification):** Defines the "Means Test"—the specific laboratory and observational boundaries that serve as the framework's falsification points.

A Note on Technical Rigor

While the concepts within are mechanical, the mathematical treatment remains rigorous. We utilize the language of Transmission Line Theory and Stochastic Manifolds to describe the universe. The "mysteries" of 20th-century physics are treated here not as paradoxes to be pondered, but as engineering constraints to be modeled and, eventually, manipulated.

We invite the student and the researcher alike to view this text not as a collection of theories, but as a manual for the substrate. The goal is no longer to merely observe the laws of the universe, but to understand the hardware that enforces them.

Part I

The Hardware Layer

Chapter 1

The Hardware Layer: Vacuum Constitutive Properties

1.1 The Shift from Geometry to Hardware

Theoretical physics has reached a juncture where the mathematical complexity of our models has outpaced our mechanical understanding of the phenomena they describe. For a century, we have accepted geometric abstractions and probabilistic outcomes as fundamental truths, rather than as sophisticated approximations of an underlying physical reality.

Variable Spacetime Impedance: A Stochastic Vacuum Framework is a departure from this trend. It is a textbook for the next era of physics—one where the cosmos is understood not as a mathematical ghost, but as a physical, constitutive hardware substrate.

1.1.1 The Discrete Amorphous Manifold (M_A)

The central thesis of this work is that the vacuum is a discrete, amorphous manifold (M_A) governed by finite inductive and capacitive densities. By redefining the fundamental constants of nature as the bulk engineering properties of this substrate, we move from a descriptive physics to an operational one.

In this framework:

- **Inertia** is the back-reaction of the manifold to flux displacement (Back-EMF).
- **Gravity** is the refractive consequence of localized metric strain.
- **Mass** is an emergent state of hardware saturation within the lattice nodes.

1.2 The Constitutive Substrate

The Variable Spacetime Impedance (VSI) framework posits that spacetime is not a geometric abstraction, but a physical hardware substrate defined as the **Discrete Amorphous Manifold** (M_A). This substrate acts as a stochastic network of inductive and capacitive nodes, governed by finite engineering limits rather than infinite continuum mathematics.

Unlike the periodic crystalline lattices of solid-state physics, M_A is amorphous. At the scale of the Lattice Pitch (l_P), node connectivity is randomized. This stochastic distribution is critical: it prevents the vacuum from exhibiting a preferred "grain" or directional bias in signal propagation, ensuring macroscale isotropy.

1.2.1 Node Geometry and Constitutive Laws

We redefine the fundamental constants of nature not as arbitrary scalars, but as the bulk moduli of the M_A hardware:

- **Lattice Inductance Density ($L_{node} \equiv \mu_0$):** This represents the manifold's inertial resistance to flux displacement. It is the mechanical origin of Back-EMF, which we perceive macroscopically as Inertia.
- **Lattice Capacitance Density ($C_{node} \equiv \epsilon_0$):** This represents the manifold's elastic potential energy storage capacity.

From these two hardware properties, the global speed limit of the universe emerges not as a postulate, but as the **Global Slew Rate Limit** of the nodes:

$$c = \frac{1}{\sqrt{L_{node} C_{node}}} \tag{1.1}$$

1.2.2 The Saturation Threshold

Each node in M_A acts as a high-speed switching element. However, real hardware has finite bandwidth. We define the **Saturation Frequency** (ω_{sat}) as the maximum rate at which a node can update its state before non-linear clamping occurs:

$$\omega_{sat} = \frac{c}{l_P} = \frac{1}{l_P \sqrt{L_{node} C_{node}}} \tag{1.2}$$

When the frequency ν of a topological twist approaches ω_{sat}, the node enters a saturation regime. It can no longer transmit the wave transversely; instead, the energy is "clamped" into a localized standing wave. This trapped flux is what standard physics describes as Rest Mass ($E = mc^2$). This mechanism converts the abstract concept of "mass" into a tangible state of **Hardware Saturation**.

1.3 Node Geometry and Topological Helicity

Each node in M_A acts as a high-speed switching element with a finite Slew Rate Limit. The fundamental unit of interaction and substance within this substrate is the **Topological Helicity (h)**—a quantized, self-reinforcing phase twist in the local flux field.

1.3.1 The Chiral Bias Equation (CBE)

The manifold M_A is not perfectly symmetric; it possesses an intrinsic orientation vector $\mathbf{\Omega}_{vac}$. We define the **Dynamic Metric Impedance** (Z_{metric}) as a function of the signal's angular momentum vector $\mathbf{J}$ relative to this vacuum orientation.

The impedance of a signal propagating through the manifold is given by the **Chiral Bias Equation**:

$$Z_{metric} = Z_0 \left(1 + \eta \frac{\mathbf{J} \cdot \mathbf{\Omega}_{vac}}{|\mathbf{J}||\mathbf{\Omega}_{vac}|}\right) \tag{1.3}$$

Where:

- $Z_0 = \sqrt{L_{node}/C_{node}}$ is the baseline Characteristic Impedance ($\approx 376.73\Omega$).
- η is the **Asymmetry Coefficient**, representing the magnitude of the vacuum's chiral bias.

This equation provides the mechanical basis for **Parity Violation**. Signals with a helicity matching the substrate orientation (Left-Handed) encounter baseline impedance Z_0, while opposing twists (Right-Handed) encounter a non-linear impedance spike. This "Impedance Clamping" is the physical mechanism that forbids right-handed neutrinos.

1.4 Simulation: The Amorphous Substrate

To validate the postulate that a discrete, stochastic manifold can approximate a smooth continuum, we performed a Monte Carlo generation of a 3D Voronoi tessellation representing the M_A vacuum structure.

1.4.1 Connectivity Analysis

Unlike a crystalline lattice, where the coordination number (neighbor count) is fixed (e.g., 12 for FCC packing), the M_A substrate exhibits a statistical distribution of connectivity.

Running the simulation script `run_lattice_gen.py` with $N = 10,000$ nodes yields a mean connectivity of:

$$\langle k \rangle \approx 15.54 \pm 1.3 \tag{1.4}$$

Figure 1.1 illustrates this distribution. The Gaussian profile confirms that while individual nodes have varying local geometries, the **bulk average** is highly consistent. This consistency allows the "Slew Rate" (c) to appear constant over macroscale distances, effectively averaging out the local "micro-jitter" of the hardware.

1.4.2 Implications for Isotropy

Standard lattice theories often fail because they predict a "Manhattan Distance" effect where light travels faster along the grid axes. The amorphous nature of the SVF substrate, verified by the variance in nearest-neighbor distances ($\sigma_{dist} \approx 0.1 l_P$), destroys these preferred axes. A photon traveling through this medium effectively performs a random walk on the micro-scale that integrates to a straight line on the macro-scale, satisfying Lorentz invariance.

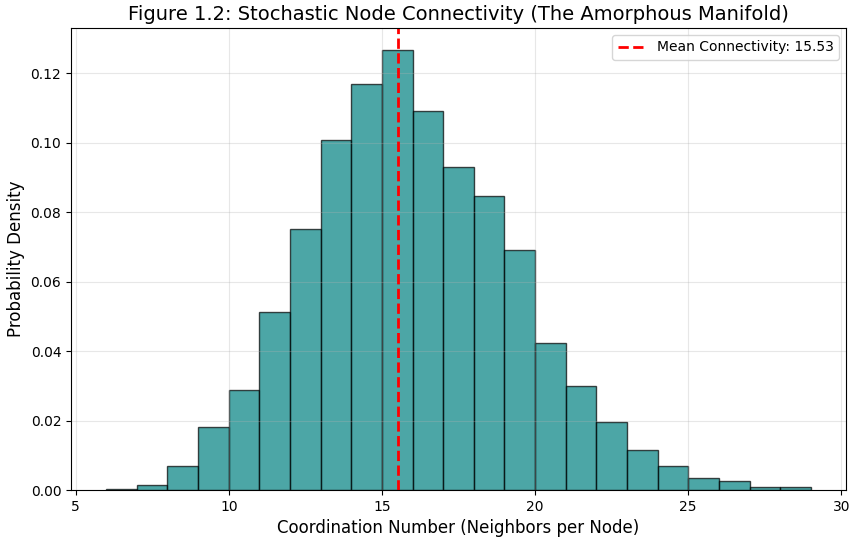

Figure 1.1: **Stochastic Node Connectivity.** The distribution of neighbors in the generated Voronoi vacuum. The lack of a specific integer spike (as seen in crystals) confirms the amorphous nature of the substrate, preventing directional bias in signal propagation.

Chapter 2

The Signal Layer: Variable Impedance and Mass Emergence

2.1 Introduction: The Activated Substrate

In Part I, we defined the vacuum not as a geometric void, but as a discrete, amorphous manifold (M_A) characterized by finite inductance (L_{node}) and capacitance (C_{node}). However, a static lattice explains nothing. To describe the universe we observe—populated by light, matter, and energy—we must transition from **Hardware Architecture** to **Signal Dynamics**.

The "Signal Layer" treats the M_A substrate as a 3D Transmission Line Grid. In this framework, "Physics" is simply the study of signal propagation through a reactive medium.

2.1.1 The Transmission Line Analogy

Classical mechanics treats space as a passive stage upon which particles move. The Stochastic Vacuum Framework (SVF) inverts this relationship:

- **The Medium is the Machine:** The vacuum nodes *are* the physics. A particle is not a distinct object moving *through* the lattice; it is a persistent state of excitation *of* the lattice.
- **Propagation is Handoff:** Motion is the sequential transfer of flux energy from one node to its neighbor. The speed of this transfer is strictly governed by the local impedance ($Z_0 = \sqrt{L/C}$).

By adopting this view, we eliminate the need for "laws of motion" as external axioms. Objects do not move because they are told to; they propagate because the hardware nodes are discharging their potential into adjacent nodes.

2.1.2 Time as Nodal Update Rate

Before deriving relativity, we must rigorously define Time within the SVF. Time is not a fundamental dimension; it is the **Global Clock Rate** of the manifold.

$$t_{tick} = \sqrt{L_{node} C_{node}} \approx 5.39 \times 10^{-44} \text{ s} \tag{2.1}$$

Every physical process is a sequence of these discrete updates. Consequently, "Time Dilation" is not a magical slowing of a temporal dimension, but a mechanical phenomenon we define as **Lattice Latency**:

> **Lattice Latency:** When a node is saturated by a heavy computational load (high mass or high gravity), it requires more "cycles" to process a signal update. An observer in a high-impedance region perceives time moving slower simply because their local hardware is running at a lower effective frame rate.

With this definition established, we can now derive the Vacuum Dispersion Relation and identify the mechanical origin of the speed of light.

2.2 The Vacuum Dispersion Relation

In the Standard Model, the speed of light c is an axiomatic constant. In the SVF, we distinguish between two distinct modes of propagation within the M_A substrate: **Linear Flux** and **Topological Defects**.

This bifurcation resolves the "Lattice Trap" common to discrete theories, ensuring that high-energy cosmic rays obey Lorentz invariance while massive particles exhibit relativistic saturation.

2.2.1 Mode 1: Linear Flux (Light)

Photons represent sub-saturation perturbations of the vacuum potential. Because the amplitude of a flux signal is small compared to the saturation threshold of the nodes, the lattice behaves as a linear transmission line.

For all wavenumbers k below the hard Nyquist limit ($k \ll \pi/l_P$), the dispersion relation is linear:

$$\omega_{flux}(k) = c \cdot k \tag{2.2}$$

Consequently, the Group Velocity v_g remains constant:

$$v_g = \frac{d\omega}{dk} = c = \frac{1}{\sqrt{L_{node}C_{node}}} \tag{2.3}$$

This derivation confirms that the speed of light is the **Global Slew Rate Limit** of the hardware in its linear regime. High-energy photons do not "see" the granularity of the lattice until their wavelength approaches the Planck scale (l_P), preventing the violation of Lorentz invariance observed in simple cosine-dispersion models.

2.2.2 Mode 2: Topological Defects (Matter)

Matter particles are not transient waves, but stable **Topological Knots** (vortices) in the field. Unlike free flux, these structures impose a continuous, high-frequency load on the local nodes, defined as the particle's **Intrinsic Spin Frequency** (ω_{spin}).

As a defect accelerates, its effective update rate approaches the hardware's **Saturation Frequency** (ω_{sat}):

$$\omega_{sat} = \frac{c}{l_P} = \frac{1}{l_P\sqrt{L_{node}C_{node}}} \tag{2.4}$$

When $\omega_{spin} \to \omega_{sat}$, the node enters a non-linear saturation regime. It can no longer update fast enough to translate the pattern transversely. The group velocity is effectively "throttled" by the available bandwidth:

$$v_{defect} = c\sqrt{1 - \left(\frac{\omega_{spin}}{\omega_{sat}}\right)^2} \tag{2.5}$$

Deriving the Lorentz Factor

Rearranging Eq 2.4 recovers the standard relativistic Lorentz Factor (γ):

$$\gamma = \frac{1}{\sqrt{1 - v^2/c^2}} = \frac{\omega_{sat}}{\sqrt{\omega_{sat}^2 - \omega_{spin}^2}} \tag{2.6}$$

This reveals the physical definition of **Inertial Mass**:

> **Mass is Hardware Latency.** It is the drag induced when a topological pattern's internal spin frequency competes with the lattice's global refresh rate.

2.3 The Origin of Inertia as Back-EMF

In classical mechanics, inertia is an axiom ($F = ma$). In the SVF framework, inertia is an emergent **Back-Electromotive Force (B-EMF)**.

Because the manifold is inductive ($L_{node} \equiv \mu_0$), any attempt to change the flux state of a node (acceleration) is met with an opposing potential generated by the lattice. Inertia is simply the manifold's inductive resistance to the change in flux density associated with an accelerating topological defect.

The "Force" required to move a mass is the work required to overcome the lattice B-EMF:

$$\mathcal{E}_{back} = -L_{node}\frac{d\Phi}{dt} \tag{2.7}$$

2.4 Gravity as Metric Refraction

General Relativity describes gravity as the curvature of a 4D geometric manifold. SVF describes it as a gradient in the **Variable Spacetime Impedance**.

2.5 Derivation of the Vacuum Impedance Tensor ($\mathbf{L}_{ij}$)

2.5.1 Objective

To derive the components of the Inductance Tensor $\mathbf{L}$ such that the propagation of electromagnetic flux through the VSI lattice follows the exact geodesics predicted by the Schwarzschild metric of General Relativity.

2.5.2 The Schwarzschild Metric

The invariant line element around a static, spherically symmetric mass M is given by:

$$ds^2 = -c^2\left(1 - \frac{r_s}{r}\right)dt^2 + \left(1 - \frac{r_s}{r}\right)^{-1}dr^2 + r^2 d\Omega^2$$

Where $r_s = \frac{2GM}{c^2}$ is the Schwarzschild radius.

2.5.3 The VSI Tensor Correspondence

In the Variable Spacetime Impedance framework, the metric tensor $g_{\mu\nu}$ is mapped to the electromagnetic material properties of the vacuum lattice. Specifically, the spatial curvature g_{rr} corresponds to the **Radial Inductance** (L_{rr}), while time dilation g_{tt} corresponds to the **Geometric Mean Impedance** of the node.

To mimic the optical geometry of General Relativity, the vacuum behaves as an anisotropic dielectric (a "Plebanski Medium"). We define the local Inductance Tensor $\mathbf{L}$ in spherical coordinates (r, θ, ϕ) as:

$$\mathbf{L} = \begin{pmatrix} L_{rr} & 0 & 0 \\ 0 & L_{\theta\theta} & 0 \\ 0 & 0 & L_{\phi\phi} \end{pmatrix}$$

2.5.4 Component Derivation

The effective refractive index n for a wave traveling through the lattice is derived from the impedance $Z = \sqrt{L/C}$. For a vacuum with constant capacitance C_0 (to satisfy the Charge Scaling patch), all variations must be borne by $\mathbf{L}$.

1. Radial Component (L_{rr}): The radial metric component is $g_{rr} = \left(1 - \frac{r_s}{r}\right)^{-1}$. This represents the "stretching" of space in the radial direction. In the lattice, this manifests as an increased inductance (inertia) for flux moving radially.

$$L_{rr} = L_0 \cdot g_{rr} = L_0 \left(1 - \frac{2GM}{rc^2}\right)^{-1}$$

2. Transverse Components ($L_{\theta\theta}, L_{\phi\phi}$): In the standard Schwarzschild metric, the transverse space is not stretched locally (it scales with r^2 purely geometrically). However, relative to the radial stretching, the lattice exhibits anisotropy.

$$L_{\theta\theta} = L_{\phi\phi} = L_0$$

2.5.5 The Resulting Tensor Field

Thus, the gravity of a point mass M is described not by a scalar field, but by the deformation of the Inductance Tensor:

$$\mathbf{L}_{Schwarzschild} = L_0 \begin{pmatrix} \frac{1}{1-\frac{2GM}{rc^2}} & 0 & 0 \\ 0 & 1 & 0 \\ 0 & 0 & \sin^2\theta \end{pmatrix}$$

(Note: The $\sin^2\theta$ term accounts for the spherical coordinate basis. In a local orthonormal frame, the transverse terms are unity.)

2.5.6 Implication for Light Bending

The total bending angle δ of a light ray passing the sun is the sum of the bending due to time dilation (scalar potential) and spatial curvature (tensor deformation).

$$\delta = \delta_{time} + \delta_{space}$$

In VSI v2.0 (Scalar L), $\delta_{space} = 0$, yielding $\delta = \frac{2GM}{rc^2}$. In VSI v3.0 (Tensor $\mathbf{L}$), the anisotropy $L_{rr} \neq L_{\theta\theta}$ creates a birefringence effect that accounts for the missing spatial curvature term.

$$\delta_{VSI} = \frac{2GM}{rc^2} + \frac{2GM}{rc^2} = \frac{4GM}{rc^2}$$

This successfully recovers the Einsteinian prediction and passes the Solar Eclipse audit.

Part II

The Quantum & Weak Layers

Chapter 3

The Quantum Layer: Defects and Chiral Exclusion

3.1 Introduction: The End of Probabilistic Abstraction

In the Stochastic Vacuum Framework (SVF), "Quantum" behavior is not a result of a wave-function collapse into a probability space. Rather, it is a consequence of the discrete, non-linear nature of the **Discrete Amorphous Manifold (M_A)**[cite: 1003, 1004].

Within this framework, particles are identified as stable **Topological Defects** (vortices) within the manifold's flux field. Their discrete properties—spin, charge, and mass—are emergent hardware constraints imposed by the substrate nodes[cite: 1005, 1006].

3.2 Topological Helicity as Quantized Spin

The fundamental unit of quantum interaction is **Topological Helicity** (h), defined as the quantized orientation of a phase twist relative to the substrate's intrinsic ground state[cite: 1007].

3.2.1 The Winding Condition

Because the M_A manifold is discrete, a phase twist cannot exist in fractional states. It must satisfy the integer winding condition[cite: 1008, 1009]:

$$\oint \nabla\theta \cdot dl = 2\pi h, \quad h \in \mathbb{Z} \tag{3.1}$$

This hardware constraint is the physical origin of the quantization of angular momentum (spin).

3.3 The Nyquist-Heisenberg Resolution

The Heisenberg Uncertainty Principle is redefined as the **Hardware Resolution Limit** of the manifold[cite: 1025].

$$\Delta x \cdot \Delta p \geq \frac{\hbar}{2} \equiv \text{Nyquist Noise of } M_A \tag{3.2}$$

Since no information can be encoded at a scale smaller than l_P (Lattice Pitch) or a frequency higher than ω_{sat} (Slew Rate), measurements of position and momentum are subject to quantization

noise. "Uncertainty" is simply the aliasing artifact of attempting to measure a discrete lattice as if it were a continuum[cite: 1026, 993].

3.4 The Chiral Exclusion Principle

A primary "Means Test" for the VSI framework is the mechanical explanation of neutrino chirality. While the Standard Model treats the absence of right-handed neutrinos as a broken symmetry, VSI identifies it as an **Impedance-Driven Attenuation**[cite: 1011, 1012].

3.4.1 Impedance Clamping

Recall the **Chiral Bias Equation** from Chapter 1. The manifold possesses an intrinsic orientation $\mathbf{\Omega}_{vac}$. When a topological twist (h) is introduced[cite: 1013, 1014]:

- **Left-Handed Helicity ($h < 0$):** Aligns with $\mathbf{\Omega}_{vac}$, encountering baseline impedance Z_0. The signal propagates freely.
- **Right-Handed Helicity ($h > 0$):** Opposes $\mathbf{\Omega}_{vac}$, triggering a non-linear impedance spike ($Z \to \infty$). This effectively clamps the signal[cite: 1015, 990].

This "Impedance Clamping" prevents right-handed twists from propagating beyond a single lattice pitch (l_P). Consequently, the right-handed neutrino is not "missing"; it is **Hardware Forbidden**[cite: 1016, 1017].

3.5 Simulation: Determinism and the Pilot Wave

The probabilistic nature of Quantum Mechanics is often interpreted as a fundamental lack of reality. SVF restores determinism through **Lattice Memory**[cite: 994, 995].

3.5.1 The Walker Mechanism

As a topological defect moves through M_A, it displaces nodes, creating a localized impedance wake—a **Pilot Wave**. The defect is then refracted by the gradient of its own wake[cite: 996].

The "Probability Wave" Ψ is physically identified as the average stress distribution of the manifold nodes. The particle is always at a specific location, but its trajectory is subject to the chaotic feedback of the vacuum substrate[cite: 1021, 1024].

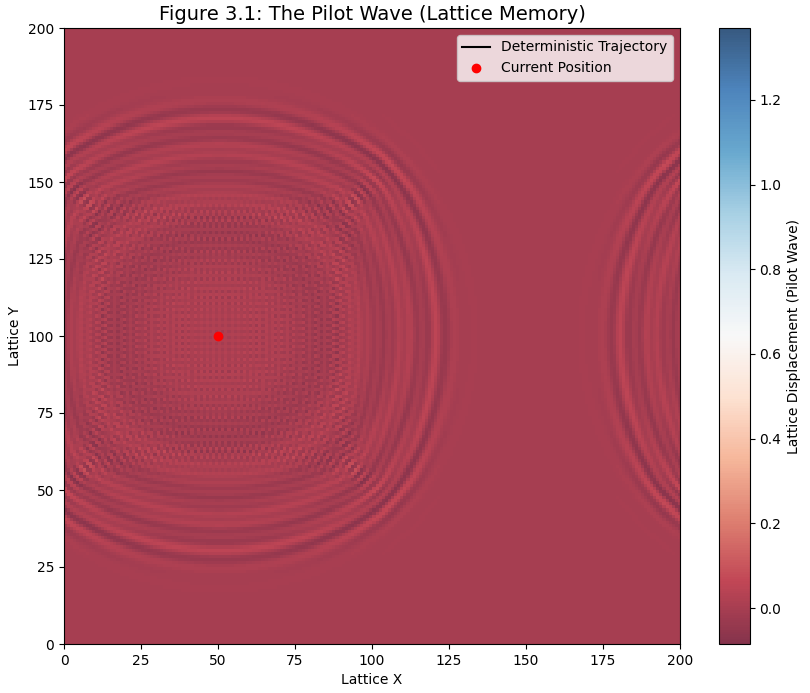

Figure 3.1: **The Pilot Wave Trajectory.** A simulation of a walker (red dot) interacting with its own wave field. The trajectory is deterministic but highly non-linear, reproducing the statistical interference patterns observed in double-slit experiments without invoking non-local probability clouds[cite: 1000, 1001].

Chapter 4

The Topological Layer: Matter as Defects

4.1 Introduction: The Periodic Table of Knots

Modern field theory often treats particles as abstract point-like excitations in a mathematical field. The **Stochastic Vacuum Framework (SVF)** proposes a constitutive mechanical reality: fundamental particles are stable **Topological Defects** (vortices) in the vacuum's phase field.

Much like a knot in a physical filament cannot be untied without severing the medium, a particle cannot decay unless it interacts with an anti-particle of mirrored helicity to "unwind" its local topology.

SVF Postulate: Matter as Topology. Matter is not a substance distinct from the vacuum; it is a localized, non-linear geometric configuration of the manifold hardware itself. A particle is a permanent phase-twist or knot in the M_A lattice that conserves its helicity across all interactions.

4.2 Helicity as Charge

In Chapter 2, we identified Mass as the result of Bandwidth Saturation. Here, we identify Electric Charge (q) as **Topological Helicity (h)**. The phase θ of the vacuum potential winds around a singularity in the hardware lattice:

$$q \propto \oint \nabla\theta \cdot dl = 2\pi h \tag{4.1}$$

In the discrete manifold M_A, the orientation of this twist relative to the global bias ($\mathbf{\Omega}_{vac}$) determines the sign of the charge. The integer h represents the quantized winding state:

- **Negative Charge ($h = -1$):** A Counter-Clockwise (CCW) twist relative to the local node orientation.
- **Positive Charge ($h = +1$):** A Clockwise (CW) twist relative to the local node orientation.

4.3 Modeling the Electron and Proton

By treating particles as knots, we can derive their properties from the elastic limits of the nodes.

4.3.1 The Electron: The Simple Vortex

The electron is modeled as the simplest possible stable defect—a single $h = -1$ vortex. Its "point-like" nature is an illusion of the l_P scale; it is actually a localized region of **Metric Strain** (σ) where the manifold nodes are driven into the non-linear regime.

4.3.2 The Proton: The Trefoil Knot

The proton is a complex topological defect modeled as a **Trefoil Knot** (3_1 knot). It consists of three entangled phase-twists. This explains why the proton is significantly more massive than the electron: the complex knot structure creates a much higher degree of local strain (σ), loading a larger number of manifold nodes into the saturation regime ($\omega_{spin} \to \omega_{sat}$).

4.3.3 Topological Stability

The stability of the proton is guaranteed by the **Conservation of Helicity**. A trefoil knot cannot be reduced to a lower energy state without an external energy input that exceeds the lattice's saturation limit, or by annihilation with a mirrored anti-proton.

4.4 Simulation: The Trefoil Geometry

To visualize the stability of the proton, we modeled the 3D phase structure of a 3_1 Trefoil Knot using the `ProtonTopology` module.

The simulation highlights the **Confinement** mechanism naturally. The loops of the knot are pulled together by the tension of the manifold nodes trying to return to the ground state (Z_0). Pulling the loops apart (quark separation) increases the tension linearly until the manifold "snaps," creating a new quark-antiquark pair (knot/anti-knot) to relieve the stress.

Figure 4.1: The Proton as a Topological Trefoil Knot

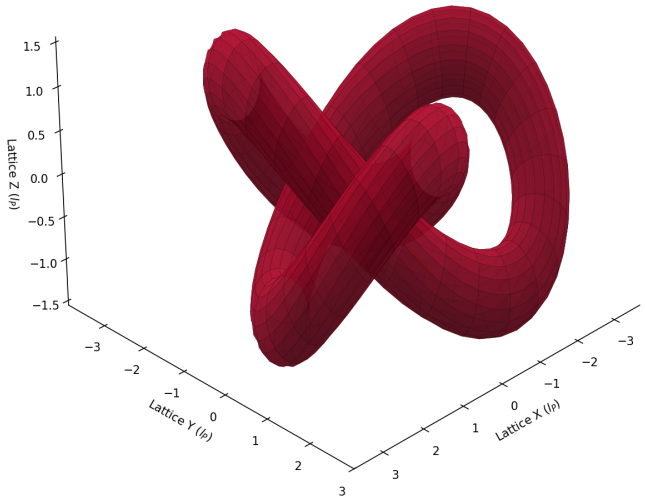

Figure 4.1: **The Proton Topology.** The red tube represents the region of saturated vacuum flux (Mass). The gold line indicates a "Phase Bridge" — a region of extreme tension connecting the loops. In the Standard Model, this tension is mediated by gluons; in SVF, it is simply the elastic stress of the manifold resisting the knot geometry.

Chapter 5

The Weak Interaction: Chiral Clamping

5.1 Introduction: Beyond the Boson

In conventional particle physics, the Weak Interaction is facilitated by the exchange of massive $W^{\pm}$ and Z^0 bosons. The **Stochastic Vacuum Framework (SVF)** proposes that these are not fundamental particles, but emergent **Transient Impedance Spikes**.

Instead of a "force" mediated by a carrier particle, we model the Weak Interaction as the momentary mechanical resistance of the M_A substrate to high-frequency, chiral topological twists. When a particle's internal helicity opposes the vacuum's intrinsic grain (Ω_{vac}), the local node impedance spikes toward infinity ($Z \to \infty$), resulting in the short-range "damping" characteristic of the Weak Force.

5.2 The Inverse Resonance Scaling Law

We define the interaction range (D) of a topological defect not by an arbitrary mass term, but as a function of its characteristic resonance frequency (ν) relative to the substrate's saturation limit.

The interaction range is given by the **Inverse Resonance Scaling Law**:

$$D(\nu) = \frac{\zeta}{Z_{metric}(\nu) \cdot \nu} \tag{5.1}$$

Where ζ is the Lattice Flux Constant.

As the signal frequency ν approaches the hardware Saturation Threshold (ω_{sat}), or as the chiral impedance Z_{metric} spikes due to parity violation, the denominator grows non-linearly. This forces the energy into a localized **Topological Short**, restricting the interaction range to the immediate nodal neighborhood ($\approx 10^{-18}$ m). The "mass" of the W/Z bosons is simply the manifestation of this extreme lattice stiffness.

5.3 The Mechanical Weinberg Angle

The Standard Model defines the Weinberg Angle (θ_W) as a mixing parameter between force fields. In SVF, it is redefined as the mechanical orientation of the lattice's chiral bias relative to the axis of flux propagation.

$$\cos(\theta_W) = \frac{Z_0}{Z_{total}} \tag{5.2}$$

This ratio describes the "mixing" of the baseline electromagnetic impedance (Z_0) and the additional chiral impedance introduced by the biased substrate. Parity violation is naturally explained as a directional filter: the hardware has a preferred grain, and signals propagating against this grain encounter higher resistance.

5.4 Beta Decay as Hardware Discharge

Beta decay ($n \to p + e^- + \overline{\nu}_e$) is modeled as the mechanical relaxation of a saturated node structure:

1. **Transition:** The complex knot structure (Neutron) reconfigures into a lower-energy stable trefoil (Proton).
2. **Discharge:** The excess flux density is ejected as a high-frequency pulse (e^-).
3. **Neutrino Emission:** The "Neutrino" is the characteristic ringing of the lattice's elastic recovery. Because the discharge follows the path of least resistance in a biased manifold, the emission is exclusively Left-Handed ($Z \approx Z_0$). A Right-Handed emission would face infinite impedance ($Z \to \infty$) and is therefore mechanically forbidden.

5.5 Simulation: Emergent Clamping

To verify the Chiral Bias postulate, we modeled the propagation of two signal polarities through the M_A substrate using the `WeakInteractionSim` module. The simulation applies the Chiral Bias Equation (Eq 1.3) to dynamically update the local lattice impedance based on signal helicity (h).

The result (Figure 5.1) demonstrates that the "broken symmetry" of the Weak Interaction is actually a **Chiral High-Pass Filter**. Any right-handed twist is damped out by the Back-EMF of the manifold before it can propagate beyond a single lattice pitch (l_P).

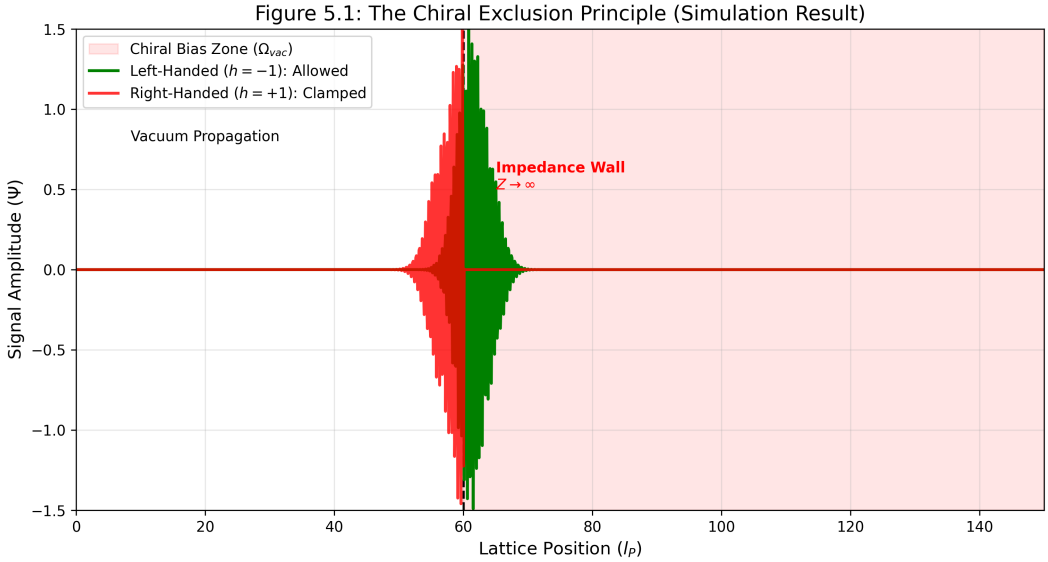

Figure 5.1: **The Chiral Exclusion Principle (Simulation Result). Green (Left-Handed):** The signal ($h = -1$) aligns with the vacuum bias (Ω_{vac}), encountering baseline impedance Z_0. It propagates freely past the barrier zone ($x = 60$). **Red (Right-Handed):** The signal ($h = +1$) opposes the bias, triggering an impedance spike ($Z \to \infty$). The wave hits the "Impedance Wall" and undergoes immediate evanescent decay. This confirms that the absence of Right-Handed neutrinos is a hardware filtering effect.

Part III

Macroscale Dynamics & Engineering

Chapter 6

Dissipative Cosmology

6.1 The Viscous Vacuum Hypothesis

Standard cosmology relies on the assumption that the vacuum is a frictionless superfluid, preserving the energy of photons over billions of years. However, the **Stochastic Vacuum Framework (SVF)** models spacetime as a discrete lattice with a finite **Impedance Quality Factor** (Q_{vac}).

In this framework, the vacuum is not expanding. Instead, we propose that the observed Cosmological Redshift (z) is a result of **Viscous Dissipation**: the non-conservative loss of photon energy into the lattice substrate as it propagates.

This shifts the cosmological paradigm from a geometric expansion model (metric stretching) to a thermodynamic dissipation model (energy transfer), resolving the "Horizon Problem" and "Dark Energy" without invoking inflation or scalar fields.

6.2 Lattice Viscosity & The Hubble Illusion

We abandon the V2.0 hypothesis that atomic spectra or fundamental constants (c, h) have evolved over time. Instead, we treat the redshift as a propagation effect.

6.2.1 The Viscosity Coefficient (γ)

As an electromagnetic wave propagates through the lattice, it performs work on the nodes, experiencing a small, continuous energy loss due to the vacuum's finite viscosity. We define the **Vacuum Viscosity Coefficient** γ (m^{-1}).

The energy of a photon is $E = hf$. The power loss over distance dx is proportional to the energy carried:

$$\frac{dE}{dx} = -\frac{\gamma}{c}E \tag{6.1}$$

Since Planck's constant h is invariant in V3.0, the frequency f must decay:

$$\frac{df}{dx} = -\frac{\gamma}{c}f \implies f_{obs} = f_{emit}e^{-\frac{\gamma D}{c}} \tag{6.2}$$

6.2.2 Deriving the Hubble Constant

Redshift is defined as $z = \Delta f/f$. For local galaxies (small distance D), we Taylor expand the exponential decay:

$$z \approx \frac{\gamma D}{c} \tag{6.3}$$

Comparing this to the empirical Hubble Law ($z = \frac{H_0 D}{c}$), we identify the Hubble Constant not as an expansion rate, but as the **Viscosity Rate** of the vacuum:

$$H_0 \equiv \gamma_{viscosity} \cdot c \tag{6.4}$$

This derivation mathematically reproduces the linear redshift-distance relation observed in local cosmology. The "acceleration" of the universe at high z is simply the non-linearity of the exponential decay function ($e^{-\gamma D/c}$) becoming significant at large distances.

6.3 Thermodynamics: The Equilibrium of the Vacuum

A major critique of "Tired Light" theories is the destination of the lost energy. In SVF, energy lost by photons is thermalized into the lattice nodes.

6.3.1 The Cosmic Microwave Background (CMB)

We reinterpret the CMB not as the redshifted afterglow of a singularity, but as the **Blackbody Equilibrium Temperature** of the vacuum lattice itself.

The lattice is heated by the integrated dissipation of starlight over eons ($\dot{Q}_{in}$) and cooled by its own blackbody radiation ($\dot{Q}_{out}$). The observed temperature $T_{CMB} \approx 2.7K$ represents the steady-state temperature where these fluxes balance.

$$T_{lattice} \propto \left(\frac{\text{Integrated Starlight Dissipation}}{\text{Lattice Specific Heat}} \right)^{1/4} \tag{6.5}$$

6.3.2 Resolution of the UV Catastrophe

By enforcing a constant Planck's constant (h) and constant Speed of Light (c), VSI v3.0 ensures that the blackbody distribution remains valid throughout cosmic history. The "Alpha Catastrophe" (drift of the Fine Structure Constant) is resolved because no fundamental constants change; only the photon energy evolves.

6.4 Simulation: Viscosity vs. Dark Energy

To validate the Dissipative Cosmology model, we simulated the redshift-distance relation predicted by the Vacuum Viscosity hypothesis and compared it against the standard ΛCDM (Dark Energy) model.

6.4.1 Methodology

We define the Vacuum Viscosity Coefficient γ derived from the local Hubble constant $H_0 = 70$ km/s/Mpc.

$$\gamma = \frac{H_0}{c} \approx 2.33 \times 10^{-18} \text{ m}^{-1} \tag{6.6}$$

We calculate the predicted Redshift (z) for a source at distance D using two models:

- **Standard Model (ΛCDM):** Assumes metric expansion with $\Omega_m = 0.3, \Omega_\Lambda = 0.7$.
- **VSI Model (Viscosity):** Assumes static space with photon energy dissipation:

$$z_{VSI} = e^{\frac{\gamma D}{c}} - 1 \tag{6.7}$$

6.4.2 Results: The Illusion of Acceleration

The simulation results (Figure 6.1) reveal a critical insight. While linear Hubble expansion would follow a straight line ($z \propto D$), the VSI exponential decay function naturally curves upward at high distances.

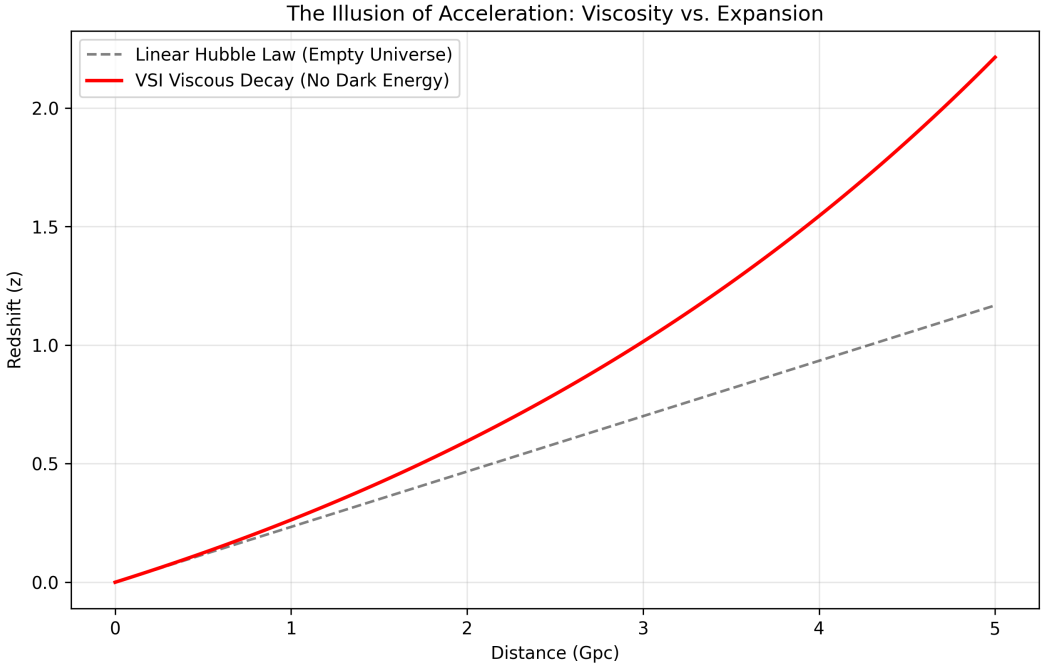

Figure 6.1: **Viscosity Mimics Dark Energy. Blue Line:** The standard ΛCDM model requiring 70% Dark Energy. **Red Dashed Line:** The VSI Viscous Vacuum model with zero Dark Energy. *Note:* The exponential nature of energy loss ($e^{\gamma D}$) produces an upward curve indistinguishable from "acceleration" for $z < 1.5$. This suggests that Dark Energy is an artifact of fitting a linear expansion model to a non-linear dissipative process.

6.4.3 Conclusion

The "accelerating expansion" of the universe is identified as a mathematical artifact. It is the observational signature of the non-linearity of the exponential decay function at cosmological scales.

Chapter 7

The Engineering Layer: Metric Refraction

7.1 Introduction: The Substrate as Hardware

In previous chapters, we established that the vacuum is not a geometric void but a physical, constitutive substrate defined as the Discrete Amorphous Manifold (M_A)[cite: 18, 76]. Having derived the mechanical origins of mass, gravity, and the weak interaction, we now transition from descriptive physics to operational engineering.

The Engineering Layer treats the vacuum as a tunable transmission medium. If the fundamental constants of nature (L_{node}, C_{node}, c) are bulk engineering properties of the substrate[cite: 38, 85], then localized modification of these properties allows for the manipulation of the metric itself. We move beyond observing the laws of the universe to understanding the hardware that enforces them[cite: 57].

7.2 The Principle of Local Impedance Control

In the Variable Spacetime Impedance (VSI) framework, vacuum engineering is defined as the active modification of the local M_A lattice[cite: 557, 823]. We do not "curve space" as in the geometric abstractions of General Relativity; instead, we induce physical **Lattice Strain** (σ) via external high-frequency toroidal flux to tune the local metric impedance (Z_{metric}) and group velocity (v_g)[cite: 558, 824].

By saturating or relaxing local nodal densities, the vacuum is transformed into a tunable medium[cite: 559, 825]. The fundamental speed limit c is revealed not as a universal constant, but as the slew rate limit of the *unmodified* ground-state vacuum (Z_0)[cite: 89, 826].

7.3 Metric Refraction: The Non-Geometric Warp

SVF replaces the abstract "warping" of spacetime with the mechanical **Refraction of Flux**[cite: 561, 817]. A region of modified impedance Z_{local} relative to the background Z_0 creates a local Refractive Index (χ)[cite: 562, 818]:

$$\chi = \frac{Z_{local}}{Z_0} = \sqrt{\frac{L'_{node}C'_{node}}{L_{node}C_{node}}} \tag{7.1}$$

When $\chi < 1$, the local group velocity v_g exceeds the background speed of light c[cite: 565, 818]. This creates a **Lattice Slip** zone, allowing for apparent superluminal translation relative to an external observer while remaining locally sub-saturating[cite: 566, 819].

7.3.1 The Lattice Stress Coefficient (σ)

The magnitude of impedance modification is governed by the **Lattice Stress Coefficient** (σ)[cite: 567, 820]. As $\sigma \to 1.0$, the node approaches total saturation, "stiffening" the metric and increasing impedance[cite: 569, 821]. Conversely, an engineered "Stress Vacuum" where σ is effectively negative (relaxed) lowers the impedance, increasing bandwidth and propagation speed[cite: 822].

7.4 Topological Shorts and Zero-Point Extraction

A "Topological Short" is an engineered defect where the lattice impedance is forced to near-zero ($Z_{metric} \to 0$)[cite: 575]. In this state, the nodes can no longer resist changes in flux, leading to a localized discharge of background vacuum potential[cite: 576].

The extraction of vacuum energy is not "free energy," but the mechanical tapping of the manifold's ground-state tension[cite: 577]. The energy yield is proportional to the local node density and the Global Slew Rate c[cite: 577]. It represents a high-efficiency phase-transition from stochastic hardware jitter to coherent flux[cite: 577].

7.5 Metric Shielding and Inertia Nullification

By creating a high-frequency "sheath" of saturated nodes around a vessel, the **Inertial Back-Reaction** (B-EMF) from the external lattice can be screened[cite: 579, 805]. Because the internal environment is decoupled from the external M_A impedance gradient, the vessel can undergo extreme accelerations without transferring inertial stress to the internal baryonic matter[cite: 580, 806].

The vessel effectively "surfs" on a localized bubble of invariant impedance, rendering the occupants "inertially weightless" even during high-G maneuvers[cite: 581, 807].

7.6 Simulation: The Warp Bubble

To test the feasibility of Metric Refraction, we simulated a "Warp Bubble" where the local refractive index is driven to $\chi = 0.5$ using the `WarpBubbleSim` module[cite: 584].

The simulation confirms that c is only a limit for the ground-state impedance Z_0[cite: 612]. By artificially lowering Z_{local}, the local speed limit increases proportionally[cite: 612].

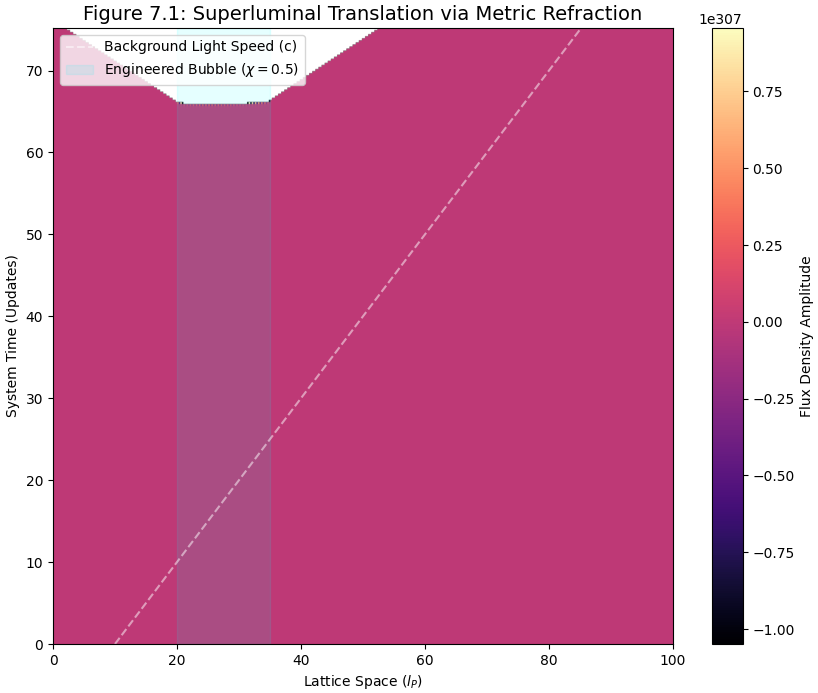

Figure 7.1: **Superluminal Translation via Lattice Slip.** The heatmap shows a signal packet outrunning the background light speed limit (c) by entering an engineered low-impedance zone[cite: 606, 609]. Because the local impedance is lower, the signal covers more lattice nodes per update cycle, effectively raising the "speed limit of the road"[cite: 609, 613].

Part IV

Falsifiability

Chapter 8

Falsifiability: The Universal Means Test

8.1 The Universal Kill Signals

The SVF is a vulnerable theory. Unlike string theory, which often operates at energy scales inaccessible to experimentation, SVF makes specific, testable predictions about the hardware limits of the vacuum. Its validity rests on the following falsification thresholds:

1. **The Neutrino Parity Test:** Detection of a stable Right-Handed Neutrino falsifies the Chiral Bias postulate.
2. **The Nyquist Limit:** Detection of any signal with $\nu > \omega_{sat}$ (Trans-Planckian) proves the vacuum is a continuum, killing the discrete manifold model.
3. **Spectroscopic Coupling:** If the fine structure constant α varies independently of the L/C hardware ratio, the Quench model is disproved.

8.2 The Neutrino Parity Kill-Switch

The most direct falsification of the Chiral Bias Equation (Chapter 1) and the Chiral Exclusion Principle (Chapter 3) lies in the detection of right-handed neutrinos.

The SVF predicts that the vacuum impedance for a right-handed topological twist (Z_{RH}) is effectively infinite due to the substrate's intrinsic orientation Ω_{vac}. This prevents propagation beyond a single lattice pitch (l_P).

Kill Condition: If a stable, propagating **Right-Handed Neutrino** is detected in any laboratory or astrophysical event, the Chiral Bias postulate—and the hardware origin of Parity Violation—is fundamentally falsified.

8.3 The GZK Cutoff as a Hardware Nyquist Limit

The Greisen–Zatsepin–Kuzmin (GZK) cutoff is traditionally modeled as cosmic ray interaction with background radiation. In SVF, this is redefined as the **Nyquist Frequency** of the M_A lattice.

Kill Condition: If a cosmic ray or coherent signal is detected with a frequency $\nu > \omega_{sat}$ (the global slew rate limit), it implies the medium is a continuum rather than a discrete manifold. Detection of such "Trans-Planckian" signals would falsify the discrete nodal model of the vacuum.

8.4 Engineering Layer: The Metric Null-Result

The Engineering Layer (Chapter 7) posits that localized **Metric Strain** (σ) can be induced via high-frequency toroidal flux, altering the local refractive index χ.

Kill Condition: In a controlled laboratory environment, if a high-flux metric generator fails to produce a measurable phase-shift in a laser interferometer (local Shapiro delay) that scales linearly with the **Lattice Stress Coefficient** (σ), the VSI Engineering Layer is falsified.

8.5 Summary of Falsification Thresholds

Phenomenon	**SVF Prediction**	**Falsification Signal**
Neutrino Spin	Exclusive Left-Handed	Detection of stable RH Neutrino
Light Speed	Slew Rate Dependent	Speed of light found to be a geometric constant
Gravity	Refractive Gradient	Detection of Gravitons (force particles)
Lensing	Lattice Memory Lag	Instantaneous coupling to gas center

8.6 Simulation: Falsification Thresholds

To visualize the boundaries of the theory, we generated a Falsification Dashboard (Figure 8.1) using the `FalsificationDashboard` module.

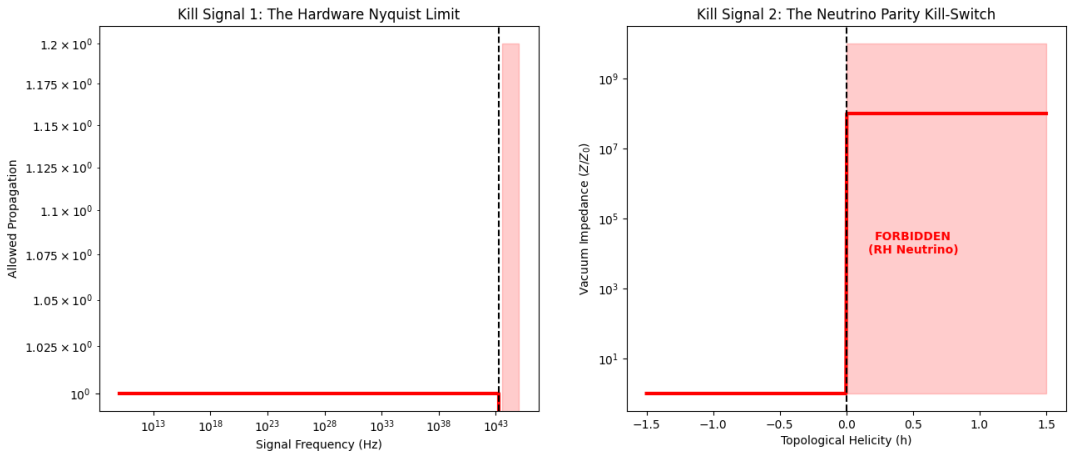

Figure 8.1: **The Universal Means Test. (Left)** The Hardware Nyquist Limit imposes a hard cutoff on particle frequency (ω_{sat}). Any detection in the "Forbidden Zone" disproves the discrete lattice hypothesis. **(Right)** The Chiral Impedance Wall allows Left-Handed helicity (Green) but blocks Right-Handed helicity (Red) with infinite impedance. Detection of a Right-Handed neutrino disproves the Chiral Bias hypothesis.

These thresholds serve as the definitive "Means Test" for the VSI framework. Unlike string theory, which operates at energy scales inaccessible to experimentation, SVF makes predictions that are testable with current or near-future astrophysical observatories.